HIGH-PERFORMANCE ULTRAVIOLET SINGLE-PHOTON DETECTION BASED ON 4H-SiC APD WITH GATED QUENCHING CIRCUITS

Baisong YE*

The detection of weak ultraviolet (UV) signals plays a critical role in high-precision applications such as quantum communication and laser ranging. We demonstrate a high-efficiency UV single-photon detection system based on a 4H-silicon carbide (SiC) avalanche photodiode (APD) integrated with a gated quenching circuit. The gating signal, characterized as a square pulse with a 5 Vpp amplitude, high-level duration, and 200 ns low-level duration, ensuring stable device operation. The system achieved a single-photon detection efficiency (SPDE) more than 20%. Key circuit parameters including APD bias and discrimination voltage were systematically investigated to optimize SPDE while mitigating the dark count rate (DCR). The results revealed that increasing the APD bias can significantly enhance SPDE, but with an exponential increase in DCR. In contrast, increasing the discrimination voltage can effectively suppress DCR, albeit with a non-linear impact on SPDE. This work establishes practical design principles for balancing sensitivity and noise performance in UV single-photon detectors, providing tailored guidelines for a range of application scenarios.

Keywords: Ultraviolet; avalanche photodiode; single-photon detection; gated quenching circuit

1. Introduction

Ultraviolet (UV) detection technology has witnessed significant progress, enabling critical applications in various fields such as biochemical analysis, astronomical observation, water purification and flame sensing [1-4]. In specialized fields including laser ranging, quantum communication, and missile plume early warning, there is a demand for detectors capable of resolving extremely weak UV signals, necessitating high-gain devices for accurate detection [5-6]. Photomultiplier tubes (PMTs) are widely used in high-gain UV detection due to their technical maturity, high gain, and low dark count rates. However, their practical adoption is limited by high cost, large physical dimensions, and the requirement for stable high-voltage supplies [7-8].

* State Key Laboratory of Intelligent Coal Mining and Strata Control, Beijing, 100013, China
CCTEG Changzhou Research Institute, Changzhou 213015, China, Tiandi (Changzhou) Automation Co., Ltd., Changzhou 213015, China, e-mail: ybswork@163.com

Avalanche photodiodes (APDs), particularly those operated in Geiger mode under high reverse bias, providing a promising alternative [9-11]. Through leveraging the avalanche multiplication effect, these devices achieve high internal gain while providing advantages such as fast response, low operating voltage (typically <200 V), compact footprint, low power consumption, high reliability, and compatibility with semiconductor integration technology. These advantages make APDs a promising replacement for PMTs in weak UV signal detection. Recent developments in UV-sensitive APDs have prioritized wide-band gap semiconductors, particularly Group III nitrides and silicon carbide (SiC), enabling direct UV detection without supplementary filters. In these materials, 4H-SiC, a well-established semiconductor with excellent material properties, has attracted significant attention from the global communities for its potential in single-photon detection applications. The development of 4H-SiC APDs began in the 1990s when J.H. Zhao's group at Rutgers University first demonstrated the internal gain of4H-SiC APDs [12]. After more than a decade of optimization, this team achieved UV single-photon detection using 4H-SiC APDs in 2005 [13]. Based on this foundation, a 4H-SiC APDs with a single-photon detection efficiency (SPDE) exceeding 20% was developed in 2014 [14]. Concurrent efforts to refine fabrication processes and testing methodologies addressed key scientific challenges, including quenching circuit design and signal extraction, thereby accelerating the practical implementation and commercialization of 4H-SiC APDs [15].

A critical challenge in single-photon detection via APDs is sustaining avalanche currents in Geiger mode, which hinder subsequent photon detection and risk thermal damage to the device. Peripheral quenching circuits are essential to reset the device bias post-avalanche, suppressing dark counts and prolonging device lifetime. In passive, active, and gated quenching circuits, gated configurations have advantages, including significantly reduced dark count rates (DCRs), compatibility with pulsed light sources, and reduced pulse probabilities. Gated quenching has become an industrial standard for Si and InGaAs APDs. However, its application in 4H-SiC APDs remains relatively unexplored, despite strong potential for high-performance applications such as laser ranging [16]. This study aims to address this gap by systematically investigating the integration of gated quenching circuits with 4H-SiC APDs. We first provide a detailed introduction to the device structure, fabrication process, and electrical characteristics (such as I-V curves and gain properties) of 4H-SiC APDs. Subsequently, we elucidate the principles of gated quenching circuit operation and evaluate how key parameters such as APD bias and discrimination voltage affect SPDE and DCR. This work aims to advance the practical deployment of 4H-SiC APDs in high-sensitivity UV detection systems.

2. Device Fabrication

Fig.1 shows a schematic cross-sectional diagram of the 4H-SiC solid-state APD fabricated for this study. The epitaxial structure is grown on a n-type 4H-SiC substrate and consists of four layers sequentially deposited from bottom to top: a 3-μm-thick p-doped region, a 0.6-μm-thick n-composite region, a 0.2-μm-thick n-doped layer, and a 0.1-μm-thick n^+ region. The doping concentrations of these four layers are $5 \times 10^{18} cm^{-3}$, $1 \times 10^{15} cm^{-3}$, $2 \times 10^{18} cm^{-3}$ and $2 \times 10^{19} cm^{-3}$, respectively. To reduce electric field non-uniformity at the mesa edge, a sloped mesa is fabricated using high-temperature reflow technology and inductively coupled plasma (ICP) etching. Then thermal oxidation was carried out at 1050°C to eliminate etching damage. The final mesa diameter was about 120 μm, with a slope of about 4°.

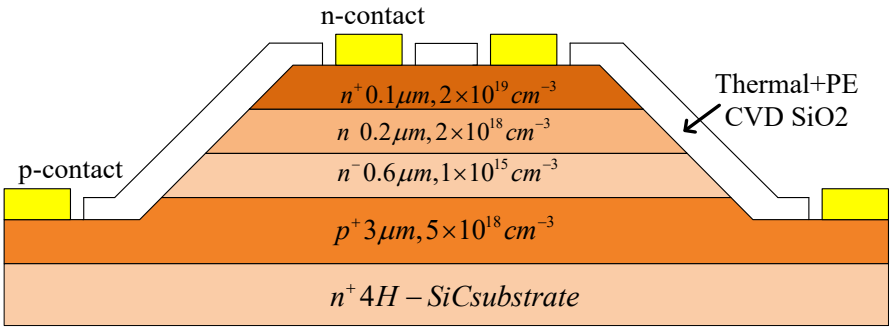

Fig. 1. Schematic cross-section of the 4H-SiC avalanche photodiode (APD) structure

3. Experiment and Discussion

The I-V characteristics of the 4H-SiC APD were measured using a Keithley 2450 source meter. The voltage output and current collection were controlled via a LabVIEW program. The dark current and photocurrent curves are shown in Fig. 2, with a 280 nm UV light-emitting diode (LED) serving as the light source. The LED has a power rating of 3 mW, a beam divergence angle of 30°, a central wavelength ranging from 275 to 280 nm, and a full width at half maximum (FWHM) of about 11 nm. The light emission is controlled via pulsed voltage modulation, wherein ultraviolet light is emitted during the high-voltage state, characterized by a duration of 20 nanoseconds. As shown in Fig.2, both the dark current and photocurrent increase significantly at about 181 V, indicating that the avalanche breakdown voltage was ~181 V. Prior to breakdown, the APD demonstrated exceptionally low dark current, remaining below 10^{-10} A at 95% of the breakdown voltage. In addition,

Fig.2 shows the variation in avalanche gain with applied bias. The avalanche gain is calculated as follows:

$$M = \frac{I_{PM} - I_{DM}}{I_P - I_D} \quad (1)$$

where I_{PM} and I_{DM} denote the photocurrent and dark current with internal gain, respectively; I_D and I_P represent the photocurrent and dark current without gain, respectively. The actual avalanche gain exceeded the maximum measurable value of 105, as shown in Fig.2. To prevent potential damage to the APD and the testing system, the photocurrent was intentionally limited during the experiment.

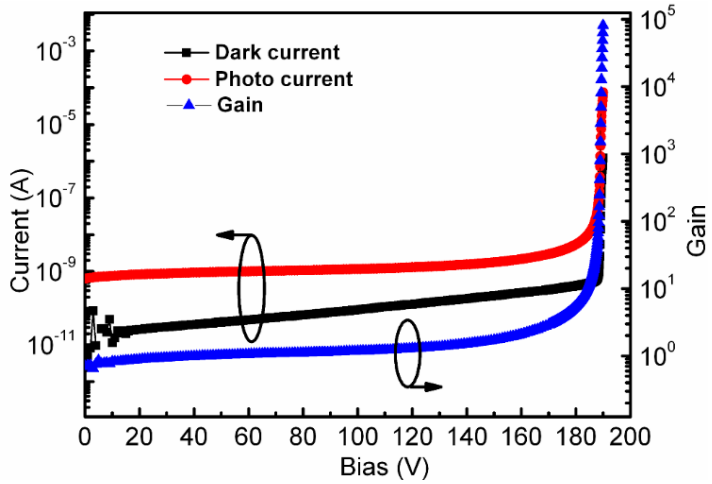

Fig. 2. Room-temperature current-voltage (I-V) characteristics and avalanche gain of the 4H-SiC APD

Fig.3 shows the block diagram of the gated quenching circuit employed in the experiment. A DC bias (Vb = 180 V) slightly below the avalanche breakdown voltage was applied to the negative terminal of APD, superimposed with a pulsed signal from a function generator. The pulse had a low-level voltage of 0 V, a high-level voltage of 5 V, a high-level duration of 40 ns, and a low-level duration of 200 ns. A 50 Ω current-sensing resistor was inserted between the APD and the bias supply, with a high-speed oscilloscope monitoring the voltage drop across this resistor. Given the high impedance of APD relative to the sensing resistor, most of the bias potential was sustained at both ends of the device. The LED light source was synchronized to the pulse bias of the APD using the same function generator. Its 20 ns pulse overlaps the APD's high-state duration of the APD. Photon emission intensity was modulated by adjusting the LED drive pulse amplitude. In each cycle, when the reverse bias (DC + pulse) of PAD exceeded Vb, incident photons or thermally generated carriers-initiated avalanche multiplication, generating a

detectable current pulse on the sensing resistor. After the pulse was terminated, the bias dropped below Vb, suppressing the avalanche current and resetting the system.

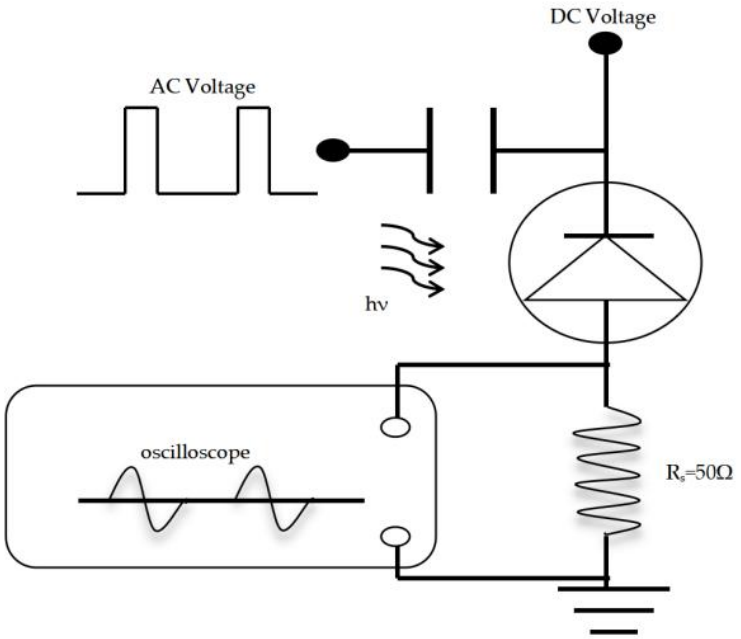

Fig. 3. Gated quenching circuit schematic of the 4H-SiC APD

APDs are commonly employed as single-photon detectors for weak ultraviolet signal detection, requiring characteristics such as high sensitivity and low noise. To assess the performance of single-photon detectors, it is essential to evaluate the SPDE and DCR of the APD. In the absence of light, the single-photon detector generates avalanche pulses due to thermal carriers, tunneling effects, and defect-related charge capture and release within the device. These pulses are known as dark counts. In the gated quenching circuit test scheme, the DCR is defined as the ratio of the number of detector counts per unit time to the repetition frequency of the gating signal. The SPDE refers to the probability that the detector responds to incident photons, defined as the ratio of experimentally measured avalanche pulses to the number of incident photons. The SPDE and DCR are influenced by the APD bias voltage. A higher bias strengthens the electric field in the avalanche region of the APD, leading to a more pronounced avalanche effect and increased device sensitivity (i.e., a higher SPDE). However, the DCR, driven by thermal effects and other factors, also increases with increasing bias, thereby impairing detection performance. As shown in Fig. 4, as the bias voltage increases, the SPDE of the 4H-SiC APD increases from less than 5% to 20%, while the DCR increases

from a10^{-6} to 10^{-2}, almost a 10,000-fold increase. In practice, carefully selecting the avalanche bias is crucial to balancing the trade-off between SPDE and DCR.

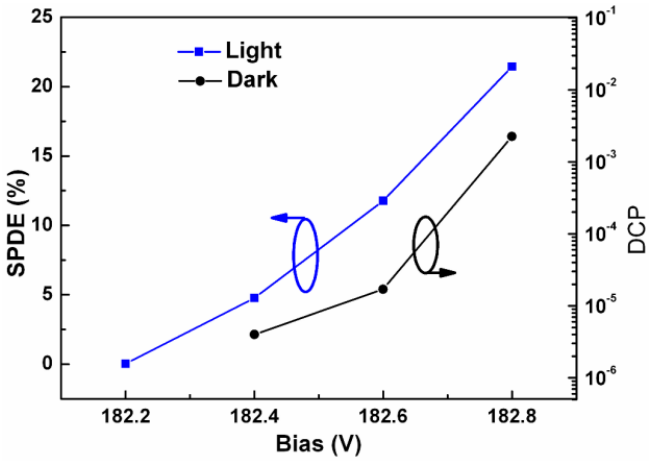

Fig. 4. SPDE and DCR as functions of avalanche bias

During the testing, we observed that the height of the avalanche pulses, whether from dark counts or photon counts, was not uniform but rather within a certain range. This phenomenon is caused by the non-uniform electric field resulting from material defects and process limitations during the fabrication of SiC-based APDs. Meanwhile, selecting an appropriate discrimination voltage can influence the performance of the APD in SPDE and DCR. As shown in Fig.5, when the discrimination voltage increases from 18 mV to 28 mV, the DCR decreases from 10^{-3} to 10^{-5}, while the SPDE decreases from about 17% to 11%. This demonstrated that a high discrimination voltage can filter out more dark pulses and photon count pulses.

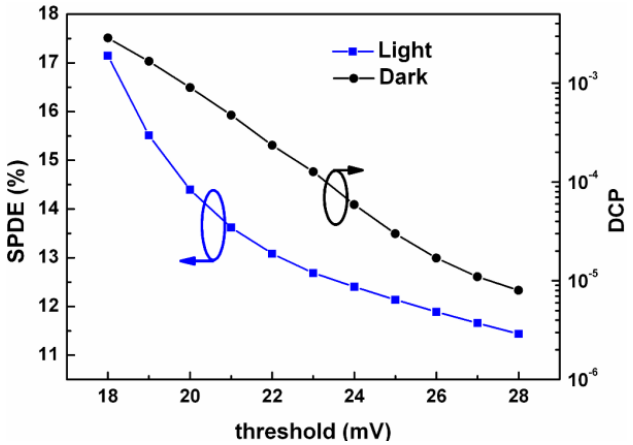

Fig. 5. SPDE and DCR as functions of discrimination voltage

Fig. 5 shows that as the discrimination voltage increases, the DCR decreases exponentially, and the SPDE could be approximately fitted by a piecewise linear relationship. When the discrimination voltage is low, SPDE decreases more rapidly. However, as the discrimination voltage increases, the slope of the SPDE decreases gradually. The relative relationship between SPDE and DCR is shown in Fig. 6. Typically, an increase in SPDE is accompanied by an increase in DCR. However, at different stages, the increase rate in DCR changes, exhibiting distinct nonlinear characteristics. In the first half of the curve, SPDE increases from about 11% to 14%, and the DCR increases sharply. In the second half, SPDE increases from about 14% to 18%, and the increase in DCR becomes more gradual. Based on the specific requirements for APD sensitivity and noise in various applications, the relationship between SPDE and DCR could help determine the appropriate bias and discrimination voltage settings.

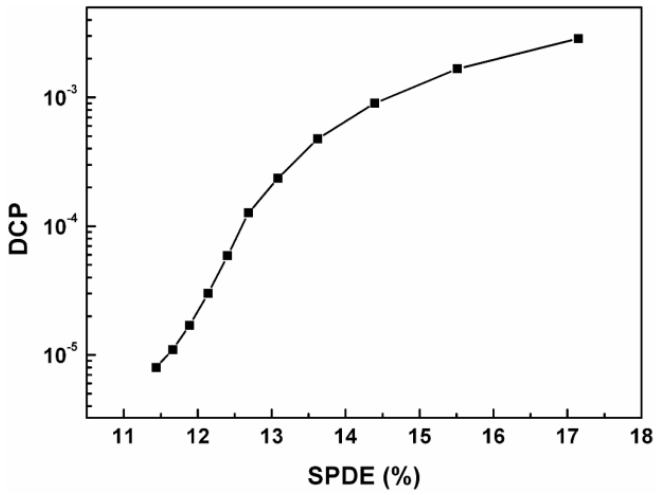

Fig. 6. DCR as a function of SPDE

4. Conclusion

This study designed and fabricated high-gain and low-dark-current APD devices based on 4H-SiC semiconductor materials and systematically charactered their optoelectronic properties. A gated quenching circuit was implemented to effectively suppress dark counts, enabling high-performance single-photon detection. The use of gate controlled quenching circuit can effectively suppress the dark count and achieve high-performance single photon detection. The influence of key circuit parameters such as APD bias voltage and threshold voltage on the SPDE and DCR was systematically investigated. Although increasing the APD bias voltage and lowering the threshold voltage both enhance SPDE, these adjustments

also reduce DCR performance. Notably, the trade-off between SPDE and DCR exhibited distinct nonlinear trends at different stages of operation, highlighting the complex interactions between these parameters. The findings of this work provide critical guidance for optimizing APD gated quenching conditions, mitigating the impact of dark counts and afterpulses on bit error rates in quantum communication and laser ranging systems. This research contributes to improved communication efficiency and a more robust operational range for single-photon detectors, thereby providing a foundation for next-generation quantum technologies and enhanced precision measurement systems.

Acknowledgments

This study was supported by Jiangsu Province Scientific and Technological Achievements Transformation Project (BA2022040); Science and Technology Innovation Venture Capital Project of Tiandi Technology Co., LTD. (2023-TD-ZD005-003).

REFERENCES

[1] *Borrego-Varillas, R., Nenov, A., Ganzer, L., Oriana, A., Manzoni, C., Tolomelli, A., Cerullo, G.,* Two-dimensional UV spectroscopy: a new insight into the structure and dynamics of biomolecules. Chemical Science, vol. 10, no. 43, pp. 9907-9921, 2019. DOI:10.1039/c9sc03871j

[2] *Fukuda, M., Yatsu, Y., Hayatsu, S., Seki, H., Joshima, S., Niwano, M., Tamura, H. et al.,* Development of UV telescope system for the astronomical observation satellite PETRE. Space Telescopes and Instrumentation 2024: Ultraviolet to Gamma Ray, vol. 13093, pp. 51-61, 2024. https://doi.org/10.1117/12.3015955

[3] *Kumari, S., Dhanda, N., Thakur, A., Gupta, V., Singh, S., Kumar, R., Thakur, P.,* Nano Ca-Mg-Zn ferrites as tuneable photocatalyst for UV light-induced degradation of rhodamine B dye and antimicrobial behavior for water purification. Ceramics International, vol. 49, no. 8, pp. 12469-12480, 2023. https://doi.org/10.1016/j.ceramint.2022.12.107

[4] *Sun, J.P., Li, X.W., Xu, X., Zhang, S.S.,* Research on ultraviolet image perception method of mine electric spark and thermal power disaster. Journal of Mine Automation, vol. 48, no. 04, pp. 1-4+95, 2022. DOI:10.13272/j.issn.1671-251x.17917

[5] *Liu, Z., An, N., Han, X., Nuñez, N. E., Jin, L., & Liu, C.,* Progress in Avalanche Photodiodes for Laser Ranging. Sensors, vol. 25, no. 9, pp. 2802, 2025. https://doi.org/10.3390/s25092802

[6] *Kasture, S., Lenzini, F., Haylock, B., Boes, A., Mitchell, A., Streed, E. W., & Lobino, M.,* Frequency conversion between UV and telecom wavelengths in a lithium niobate waveguide

for quantum communication with Yb+ trapped ions. Journal of Optics, vol. 18, no. 10, pp. 104007, 2016. DOI:10.1088/2040-8978/18/10/104007

[7] *Mozhaiko, A. A., Manninen, S. A., Mukhamedzyanova, L. V., Kuznetsov, P. A., Knyazyuk, T. V., Serebrov, A. P., Fedorov, V. V.,* Development and Study of Magnetic Shields for Neutrino Detector Photomultiplier Tubes under Neutrino-4M Experiment on PIK and SM-3 Reactors. Technical Physics, vol. 69, no. 5, pp. 1287-1295, 2024. https://doi.org/10.1134/S1063784224040261

[8] *Beavers, J., Huddleston, K., Hines, N., & McNeil, W.,* Simulation of electron transport in a catoptric photomultiplier tube concept for large rectangular scintillator crystals. Journal of Instrumentation, vol. 19, pp. P04025, 2024. DOI:10.1088/1748-0221/19/04/P04025

[9] *Fang, Y., Wang, C., & Xie, D.,* Gm-APD Lidar Distance Image Recovery Based on Intensity Image Target Edge Guidance. Journal of Physics: Conference Series, vol. 2872, no. 1, pp. 012039, 2024. DOI:10.1088/1742-6596/2872/1/012039

[10] *Liu, F., Wang, J., Wang, D., Zhou, D., & Lu, H.,* Photo-Electric response of 4H-SiC APDs at High-Level incident flux. Results in Physics, vol. 50, pp. 106608, 2023. DOI:10.1016/j.rinp.2023.106608

[11] *Zhou, X., Tan, X., Lv, Y., Wang, Y., Li, J., Song, X., Cai, S.,* Single-Photon-Counting Performance of 4H-SiC Avalanche Photodiodes With a Wide-Range Incident Flux. IEEE Photonics Technology Letters, vol. 32, no. 14, pp. 847-850, 2020. Doi: 10.1109/LPT.2020.3000271

[12] *Yan, F., Luo, Y., Zhao, J. H., & Olsen, G. H.,* 4H-SiC visible blind UV avalanche photodiode. Electronics Letters, vol. 35, no. 11, pp. 929-930, 1999. https://doi.org/10.1049/el:19990641

[13] *Xin, X., Yan, F., Alexandrove, P., Sun, X., Stahle, C. M., Hu, J., Zhao, H. J.,* Demonstration of 4H-SiC UV single photon counting avalanche photodiode. Electronics Letters, vol. 41, no. 4, pp. 212-214, 2005. https://doi.org/10.1049/el:20057320

[14] *Zhou, D., Liu, F., Lu, H., Chen, D., Ren, F., Zhang, R., & Zheng, Y.,* High-Temperature Single Photon Detection Performance of 4H-SiC Avalanche Photodiodes. IEEE Photonics Technology Letters, vol. 26, no. 11, pp. 1136–1138, 2014. DOI: 10.1109/LPT.2014.2316793

[15] *Liu, F., Yang, S., Zhou, D., Lu, H., Zhang, R., & Zheng, Y. D.,* Discrimination Voltage and Overdrive Bias Dependent Performance Evaluation of Passively Quenched SiC Single-photon Counting Avalanche Photodiodes. Chinese Physics Letters, vol. 32, no. 8, pp. 088503, 2015. DOI: 10.1088/0256-307X/32/8/088503

[16] *Du, H., Li, W., Wang, Y., Xu, W., Zhou, D., Ren, F., Lu, H.,* A Pulsed Ultraviolet Laser Positioning System Based on 4H-SiC Four-Quadrant Photodetectors. IEEE Photonics Technology Letters, vol. 36, no. 11, pp. 697-700, 2024. DOI: 10.1109/LPT.2024.3389109